Development of wavelength shifter coated reflectors for the ArDM argon dark matter detector

2009 JINST 4 P06001

(http://iopscience.iop.org/1748-0221/4/06/P06001)

JINST

PUBLISHED BY IOP PUBLISHING FOR SISSA

RECEIVED: *April 15, 2009*
ACCEPTED: *May 9, 2009*
PUBLISHED: *June 1, 2009*

Development of wavelength shifter coated reflectors for the ArDM argon dark matter detector

The ArDM Collaboration

V. Boccone,[a] P.K. Lightfoot,[e] K. Mavrokoridis,[e] C. Regenfus,[a] C. Amsler,[a] A. Badertscher,[b] A. Bueno,[c] H. Cabrera,[a] M.C. Carmona-Benitez,[c] M. Daniel,[d] E.J. Daw,[e] U. Degunda,[b] A. Dell'Antone,[a] A. Gendotti,[b] L. Epprecht,[b] S. Horikawa,[b] L. Kaufmann,[b] L. Knecht,[b] M. Laffranchi,[b] C. Lazzaro,[b] D. Lussi,[b] J. Lozano,[c] A. Marchionni,[b] A. Melgarejo,[c] P. Mijakowski,[f] G. Natterer,[b] S. Navas-Concha,[c] P. Otyugova,[a] M. de Prado,[d] P. Przewlocki,[f] F. Resnati,[b] M. Robinson,[e] J. Rochet,[a] L. Romero,[d] E. Rondio,[f] A. Rubbia,[b,1] N.J.C. Spooner,[e] T. Strauss,[b] J. Ulbricht[b] and T. Viant[b]

[a] *University of Zürich, Physik-Institut, CH-8057 Zürich, Switzerland*
[b] *ETH Zurich, Institute for Particle Physics, CH-8093 Zürich, Switzerland*
[c] *University of Granada, Dpto. de Física Teórica y del Cosmos & C.A.F.P.E, Campus Fuente Nueva, 18071 Granada, Spain*
[d] *CIEMAT, Div. de Fisica de Particulas, Avda. Complutense, 22, E-28040, Madrid, Spain*
[e] *University of Sheffield, Department of Physics and Astronomy, Hicks Building, Hounsfield Road, Sheffield, S3 7RH, U.K.*
[f] *The Andrzej Soltan Institute for Nuclear Studies, Hòza 69, 00-681 Warsaw, Poland*

E-mail: andre.rubbia@cern.ch

ABSTRACT: To optimise the design of the light readout in the ArDM 1-ton liquid argon dark matter detector, a range of reflector and WLS coating combinations were investigated in several small setups, where argon scintillation light was generated by radioactive sources in gas at normal temperature and pressure and shifted into the blue region by tetraphenyl butadiene (TPB). Various thicknesses of TPB were deposited by spraying and vacuum evaporation onto specular 3M^{TM}-foil

[1] Corresponding author.

doi:10.1088/1748-0221/4/06/P06001

2009 JINST 4 P06001

and diffuse Tetratex® (TTX) substrates. Light yields of each reflector and TPB coating combination were compared. Reflection coefficients of TPB coated reflectors were independently measured using a spectroradiometer in a wavelength range between 200 and 650 nm. WLS coating on the PMT window was also studied. These measurements were used to define the parameters of the light reflectors of the ArDM experiment. Fifteen large $120 \times 25\,\mathrm{cm}^2$ TTX sheets were coated and assembled in the detector. Measurements in argon gas are reported providing good evidence of fulfilling the light collection requirements of the experiment.

KEYWORDS: Photon detectors for UV, visible and IR photons (gas); Photon detectors for UV, visible and IR photons (vacuum); Scintillators, scintillation and light emission processes (solid, gas and liquid scintillators); Gaseous detectors

ARXIV EPRINT: 0904.0246

2009 JINST 4 P06001

Contents

1 Introduction

The ArDM experiment [1, 2] aims for the operation of a ton-scale liquid argon target for direct detection of dark matter particles scattering off nuclei with a recoil energy threshold of 30 keV. A high reconstruction sensitivity for such events depends on an efficient detection of scintillation light and ionization charge. Ionizing radiation in liquid noble gases leads to the formation of excimers in either singlet or triplet states [3, 4], which decay radiatively to the dissociative ground state with characteristic fast and slow lifetimes ($\tau_{fast} \approx 6$ ns, $\tau_{slow} \approx 1.6\mu$s in liquid argon with the so-called second continua emission spectrum peaked at 128 ± 10 nm ([5]). In room temperature argon gas at 1 bar $\tau_{slow} \approx 3.2\mu$s and the third continuum in the wavelength range between 175 and 250 nm populates most of the fast component [6–8]. Singlet and triplet states are produced with different amplitudes depending on the ionizing radiation. In addition, the phenomenon of recombination effectively transforming ionization into scintillation [9], depends on the ionization density in the medium. Based on these properties, it was shown that the relative fraction of scintillation to ionization [10] and the time structure of the argon scintillation light [11] can be used in liquid to discriminate nuclear recoils against γ and electron backgrounds which enter the sensitive fiducial region of the target.

2009 JINST 4 P06001

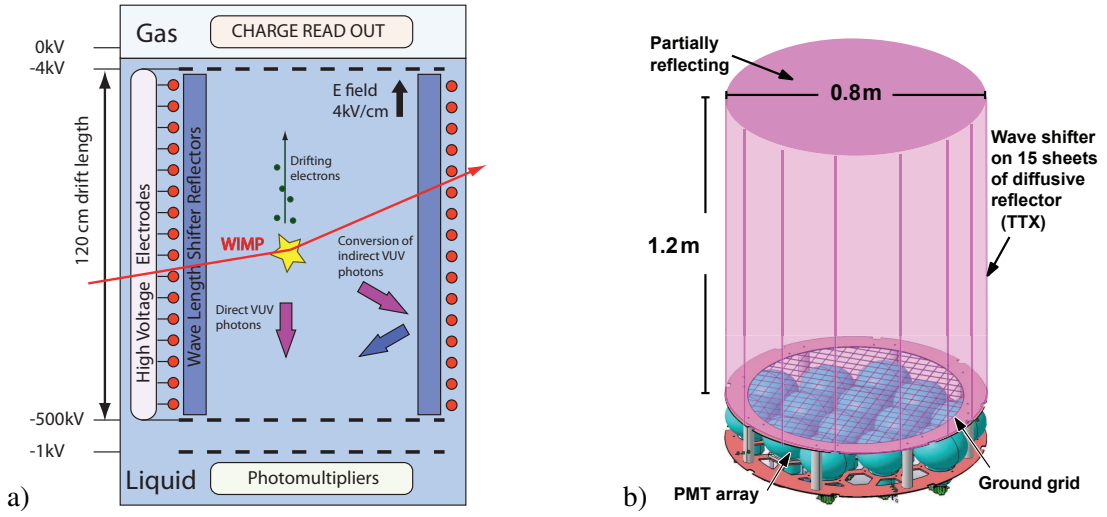

Figure 1. (left) Operation principle of the ArDM detector, (right) 3D sketch of the 83 cm by 120 cm cylindrical light detection volume.

The ArDM detector will be operated as a double phase LAr LEM-TPC [12], as is illustrated in figure 1(left). The charge readout will be situated in the gas phase at the top of the vessel, while photodetectors sensitive to single photons will be located in the liquid argon at the bottom of the apparatus. In the following, we concentrate on the light readout system.

As mentioned above, the UV scintillation light of liquid argon is below 150 nm. Since large VUV sensitive PMTs (e.g. MgF_2 windowed) are not commercially available, the use of reflectors coated with a wavelength shifter (WLS) along with standard bialkali photomultiplier tubes (PMTs) is an economical realisation of an efficient readout system.

In ArDM, the light readout system will be composed of 14 hemispheric 8" Hamamatsu R5912-02MOD-LRI PMTs, made from particularly radiopure borosilicate glass and feature bialkali photocathodes with Pt-underlay for operation at cryogenic temperatures [13]. The argon scintillation light is wavelength shifted into the range of maximum quantum efficiency (QE) of the PMT by a thin layer ($1.0\,mg/cm^2$) of tetraphenylbutadiene (TPB) evaporated onto 15 cylindrically arranged reflector sheets ($120 \times 25\,cm^2$) which are located in the vertical electric field. These sheets are made of the PTFE fabric Tetratex® (TTX), transporting the shifted light diffusively onto the PMTs (shown in figure 1 (right)). The PMT glass windows are also coated with TPB to convert directly impinging DUV photons.

In this paper, we present our investigations on TPB coating methods, sample preparation, and optimisation of TPB coating thickness on two separate reflector substrates. These results have led to the optimization of the reflector and PMT coating used for the ArDM experiment.

2 WLS, reflector material and coating techniques

2.1 The wavelength shifting chemical

We seek a fast response of the light readout system not to distort the pulse shape of the liquid argon scintillation light. Most organic wave shifting materials are well known for their fast optical re-

2009 JINST 4 P06001

sponse caused by the rapid process of radiative recombination of electron hole pairs at the benzene rings in their chemical structure. Typical well-known elements satisfying these requirements are p-Terphenyl (PTP) with an emission curve between 280 and 350 nm, diphenyloxazolyl-benzene (POPOP) between 340 and 420 nm, diphenyloxazole (PPO) between 305 and 365 nm [14], and tetraphenyl-butadiene (TPB) between 400 and 480 nm [14, 15].

We select TPB above other waveshifting compounds for the well matched emission spectrum to our bialkali photocathodes. Tetraphenyl-butadiene (TPB) coatings have been studied in [15–19] and successfully used in previous experiments (see e.g. [20, 21]). They are particularly well suited for the detection of DUV light due to the large Stokes shift of TPB [14, 15, 17, 22]. The fluorescence decay time is about 1.68 ns [22] and, since no phonons are involved, the recombination process does not slow down significantly at cryogenic temperatures. TPB coatings can be made durable with good adherence to the substrate and high resistance to mechanical abrasion. The coatings are generally not soluble in water but can be removed when necessary by using toluene, chloroform ($CHCl_3$) or other organic solvents. TPB coatings have been exposed to high vacuum conditions for very long periods of time and have shown no evidence of significant change in the detector sensitivities.

2.2 Reflector type and outgassing measurements

The presence of the strong electric field at the position of the light reflector (figure 1(left)) demands non conductive material as the substrate for the wavelength shifter. Our research focussed on the two materials ESR (Vikuiti^{TM} Enhanced Specular Reflector foil) from the company 3M^{TM} and Tetratex® (TTX) from the company Donaldson Membranes. 3M^{TM} foil is a multilayer specular reflecting polymer film and as such likely to be of high radio-purity. Its appearance is that of a polished metal although the material is non conducting. It has a specular reflection coefficient of practically 100% in a large region of the optical spectrum. TTX is an aligned polytetrafluoroethylene (PTFE) fibrous cloth and is nearly a 100% diffuse Lambertian reflector. We employ TTX in the thickness of 254 μm which is often used for wrapping crystals. A photograph of TTX cloth taken with a scanning electron microscope is shown in figure 2. Because of the manufacturing method, which relies on extrusion of polymer chains within an oil based emulsion, doubts have been raised concerning both the purity of TTX and its outgassing rate. The outgassing properties were checked with a dedicated sample of 48 g of 254 μm TTX (equivalent to 1/20 of the total amount required to line the ArDM experiment). The sample was placed within a large chamber which was evacuated. A series of measurements confirmed the good outgassing properties of TTX. The outgassing products were analysed using a mass spectrometer[1] and found to predominantly contain nitrogen and water. In order to investigate the radio-purity of TTX, samples were sent to Harwell Scientifics for analysis by inductively coupled plasma mass spectroscopy (ICP-MS). The detection limits of the instrument are 0.3, 0.4 and 500 parts per billion (ppb) for U, Th and K respectively. TTX radiopurity was found to be 1.0 ± 0.3, < 0.4 and < 500 ppb for U, Th and K concentrations respectively. Table 1 compares the results from the analysis with other data taken using the ICP-MS analysis of standard target components.

[1] MKS Spectra Microvision Plus.

2009 JINST 4 P06001

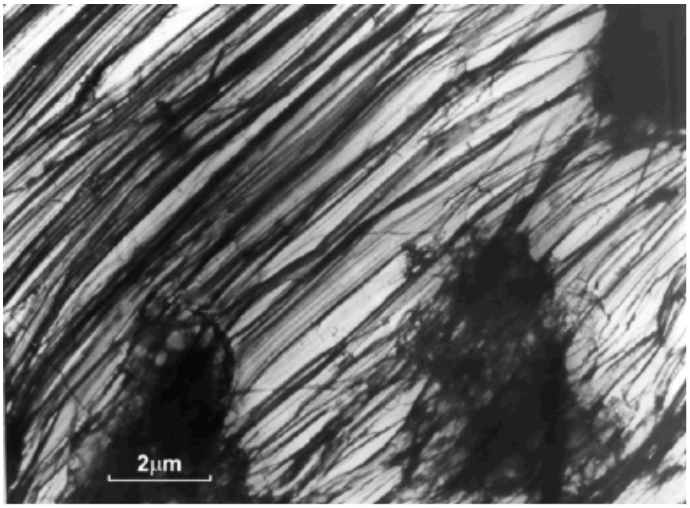

Figure 2. Photograph of a Tetratex® sample taken with a scanning electron microscope.

Table 1. TTX radio-purity compared with the radio-purity of standard target components. The reference impurity levels are based on the UK Dark Matter Collaboration internal measurements [23].

Sample	U conc. (ppb)	Th conc. (ppb)	K conc. (ppm)
Tetratex® (TTX) this paper	1.0 ± 0.3	< 0.4	< 0.5
Polyethylene	< 0.3	< 0.4	< 0.5
Copper	1.0	1.0	0.5
Steel	2.8	1.5	< 0.5
Quartz	4.0	4.0	21
Borosilicate glass	30	30	120
Molecular sieve	34	14	61
Aluminum oxide	400	16	19
Ceramic capacitor	450	400	320

2.3 Coating techniques on reflectors and PMT windows

TPB powder can be applied to a reflector or PMT window by vacuum evaporation, spraying, or by dissolving in a polymer matrix [17, 18, 24, 25]. For comparison figure 3 shows microscope photographs of evaporated and sprayed 3M^{TM} foil samples illuminated with UV light. The granular structure of the air brush method due to the formation of small crystals can easily be observed, while the coating achieved by evaporation of TPB is very uniform.

The 3M^{TM} foil samples were prepared by evaporation in a modified glass exsiccator where two electrical feedthroughs were added. Because of the low melting point of TPB (207 °C) and its chemical inertness, the requirement on the vacuum is modest. Typically a value of 10^{-4} mbar for the residual pressure was reached. A 15 mm diameter Al_2O_3 crucible is employed, being able to hold up to 1.5 g of TPB powder. Heating is provided by a tungsten filament wound around the entire height of the crucible for even heat transport. Heating power was set between 3–8 W for evaporation cycles from about 30 min to 5 hours.

2009 JINST 4 P06001

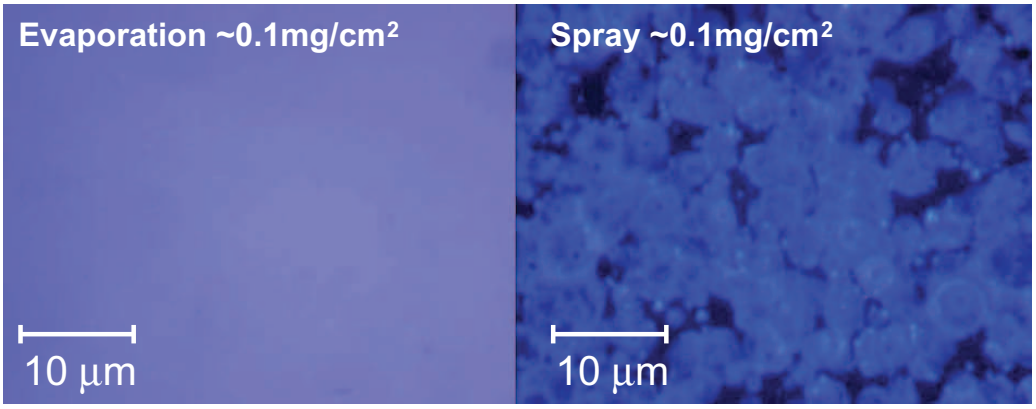

Figure 3. Surface structure of evaporated (left) and sprayed (right) TPB on 3M ^{TM} foil under the microscope, illuminated by 250 nm light.

For the rest of the measurements the vacuum evaporation of the samples was performed in a commercial Edwards model E308 evaporation chamber. Here up to 3 g of TPB powder was heated by applying 24 A current to the molybdenum sample holder. The reflector/PMT window was placed above the TPB powder at a fixed distance and the coating thickness was controlled by varying this distance and the weight of the powder.

Sprayed coatings were prepared by dissolving TPB in toluene in a ratio of 1 to 40. This solution was then airbrushed onto the substrate using 1.2 bar argon gas.

The polymer matrix coatings on PMT windows (compare also [25]) were prepared using long chain paraloid or polystyrene plastic fragments dissolved in toluene. TPB was added and dissolved isotropically. A known amount of obtained liquid was then syringed onto the substrate. The TPB concentration within the solution was varied, as was the amount of liquid applied to the substrate. The solution was left for three hours to allow the toluene to evaporate, forming clear TPB impregnated plastic.

3 Results

3.1 Method

Preliminary investigations with gaseous argon and α particle excitation at normal temperature and pressure (NTP) were described in an earlier work [8]. A typical argon scintillation pulse at NTP can be described by a sum of two exponentials with the time constants τ_1 and τ_2 for fast and slow components, respectively. The slow scintillation component can be used to measure the VUV light yield at 128 nm, however, its measured light yield and the measured decay time of the slow scintillation component τ_2 strongly depends on gas purity. This dependence is attributed to impurities destroying the long-lived triplet argon excimer state. Therefore τ_2 can be used as a measure of argon purity. In order to correct for this effect and to compare various measurements, results are plotted versus the measured value of τ_2. This method, described in [8], allows to determine the individual light yield by extrapolation to τ_{slow}=3.2 μs, corresponding to the maximum slow decay time observed in pure argon at 1 bar [26], disentangling the effect of impurities in the argon gas.

2009 JINST 4 P06001

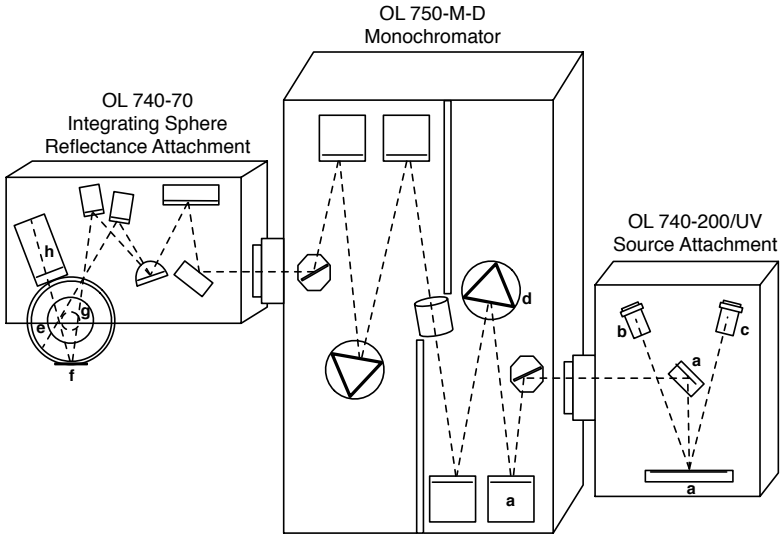

Figure 4. Schematic of the Optronics OL750 spectroradiometer. a: selecting mirror, b: quartz halogen light source, c: deuterium light source, d: diffraction grating mount, e: integration sphere, f: sample, g: silicon photo diode detector, h: light trap. Figure redrawn from the manual.

3.2 Reflection coefficient measurements of TPB coated reflectors

An Optronics OL750 spectroradiometer with an OL740-70 integrating sphere [27] was used to measure reflectance and global fluorescence from 200 nm to 700 nm for a range of samples with TPB deposited by spray, evaporation, and polymerisation over a variety of thicknesses and concentrations, and on a range of substrates. A schematic of the spectroradiometer can be seen in figure 4.

The light sources used were deuterium (200–400 nm) and quartz halogen (330–700 nm) which were calibrated with a mercury lamp. An automatic motorized monochromator allowed selecting a specific wavelength to within 1 nm. This light was directed through a small opening to be incident on a 2 cm diameter target sample within an integrating sphere whose internal surfaces were coated with PTFE. Light reflecting from the sample is then integrated within the sphere prior to being collected by a silicon photo diode detector. The absolute value of the reflection coefficient was measured by comparing light collected from a sample to that produced by a calibrated NIST registered pressed PTFE sample.[2] For diffuse reflectance measurements, the sample was positioned at an angle of 15 degrees to the incident light, and a light trap positioned at a port on the integrating sphere such that all specularly reflected light would be trapped and could not contribute to the integrated signal.

Figure 5 shows the reflectance of uncoated 3M ^{TM} foil and TTX cloth samples. The wavelength on the horizontal axis refers to the incident light wavelength, selected by the monochromator. The reflection coefficient cannot be measured in VUV (i.e. below 200 nm) with this type of spectroradiometer, because the radiation is absorbed by air. In addition, below 400 nm, most light reflected off the coated samples is shifted to a mean wavelength of 430 nm, well within the measurable region of the equipment. Relative reflection coefficients greater than one indicate here fluorescence.

[2] A calibrated sample obtained from the National Institute of Standards & Technology.

2009 JINST 4 P06001

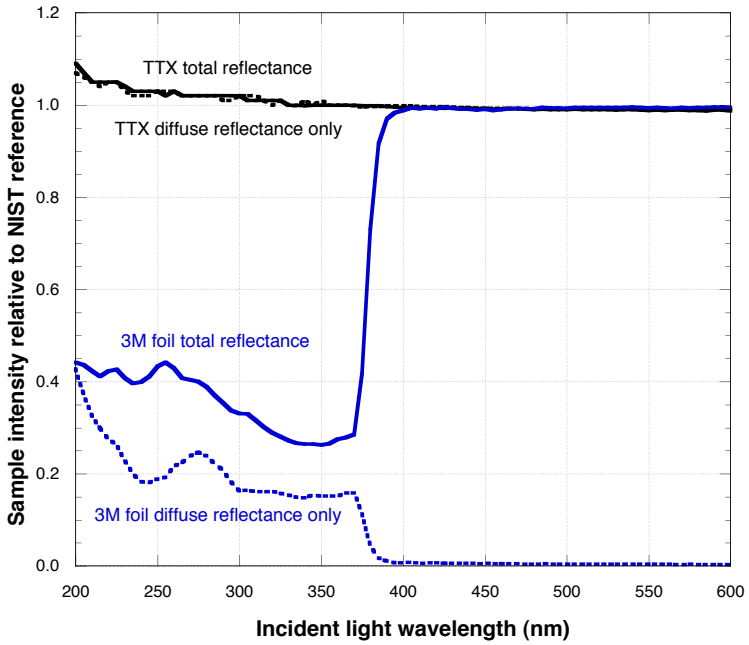

Figure 5. Comparison of total and diffuse reflection intensity for TTX and 3M ™ foil substrates relative to the NIST reference sample.

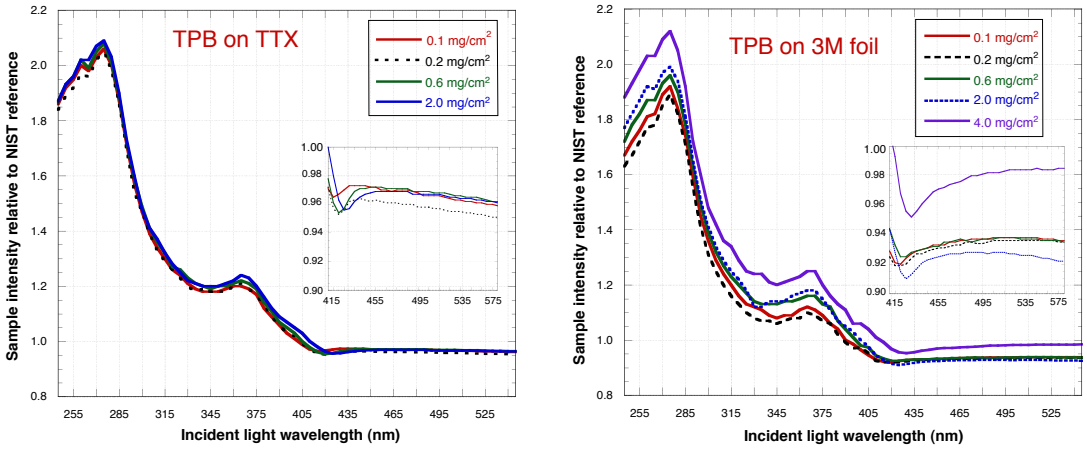

Figure 6. Total reflectance of (left) single thickness TTX cloth; (right) TPB evaporated onto 3M™ foil. The insets show an expanded scale in the wavelength range 415 to 575 nm.

As expected, light reflected from uncoated TTX is 100% diffuse, and light from 3M™ foil above 390 nm is 100% specular. Interestingly, below 370 nm light from the 3M™ foil is over 50% diffuse and this rises to 100% of its total reflectance at 200 nm.

Figure 6 presents the results for different coatings. The reflectance coefficient for TPB coated 3M ™ foil is about 93% at 430 nm and varies slightly between the thickest (4.0 mg/cm^2) and the thinnest (0.1 mg/cm^2) samples. On the other hand, evaporated TTX samples have a reflection coefficient close to 97% at 430 nm and this property is less sensitive to the TPB thickness.

2009 JINST 4 P06001

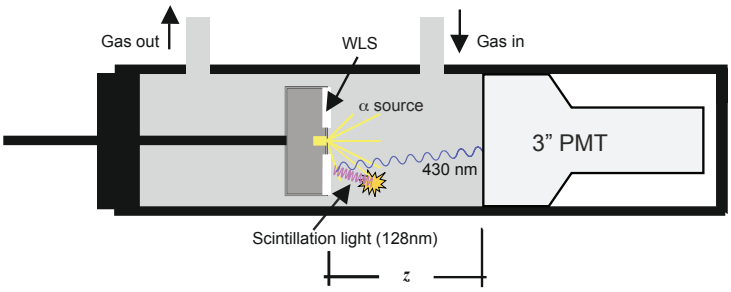

Figure 7. Setup to determine the conversion efficiency of TPB coated 3M ™ foil disks.

Diffuse and total reflectances for 3M ™ foil TPB coated samples were also studied. The maximum specular component of the thinnest sample on 3M ™ foil is $< 3\%$ and the thickest is $< 1\%$ at 430 nm. This indicates that irrespective of the TPB coating thickness, reflected light within any target will be almost completely diffuse. This result also implies that the 3M ™ foil is contributing little to the reflectivity of the sample for the thickest coatings (which on 3M ™ foil have consistently produced more light) for wavelengths between 345 and 555 nm. These measurements favor the TTX fabric as the base of our reflectors.

3.3 Conversion efficiency of a thin TPB layer on 3M ™ foil

In a first test we investigated the wave shifting efficiency of thin TPB layers on 3M™ foil with respect to their thicknesses [28]. TPB was applied onto the samples by vacuum evaporation in the above described exsiccator. A set of 13 disks of 3M™ foils (diameter 70 mm) was prepared with TPB layers ranging from 0.011 to 2.8 mg/cm^2, while a 14th disk was left untouched. The amount of TPB deposited on the disks was determined by weighing the disks before and after evaporation. During all evaporations the foils were held at constant distance to the crucible. The amount of TPB loaded in the evaporator crucible was found to be in nice linear relation to the amount of TPB on the disk after evaporation. The increase in brightness of thicker TPB layers becomes apparent under illumination with a UV lamp (300 nm). The response to 128 nm light was then determined using scintillation light from argon gas.

For this purpose the foils were mounted onto a movable holder opposite to an uncoated bialkali PMT ($z = 6.7$ cm) in a black lined tube (figure 7) which was connected to a high purity (99.9999%) argon gas system. Without prior pumping the gas flow improves gradually the argon purity in the chamber while the scintillation light from ^{241}Am α-particles is recorded continuously.[3] The average photoelectron number from α signals of individual data sets was then plotted vs. the measured value of τ_2, the decay time of the slow scintillation component (See figure 8(left)). Every line corresponds to a different disk and hence a different TPB thickness. Deviations of measurement points from the lines are caused by not stable starting conditions (mainly air humidity) and uneven increase of the argon purity among the taking of the different data sets.

The lines were fitted to a common intersection point which was left floating. The colour map represents the χ^2-values of this point (red = smallest χ^2). The abscissa values of this point agree

[3]The total deposition of α energy occurs within 4 cm in 1 bar of gaseous argon.

2009 JINST 4 P06001

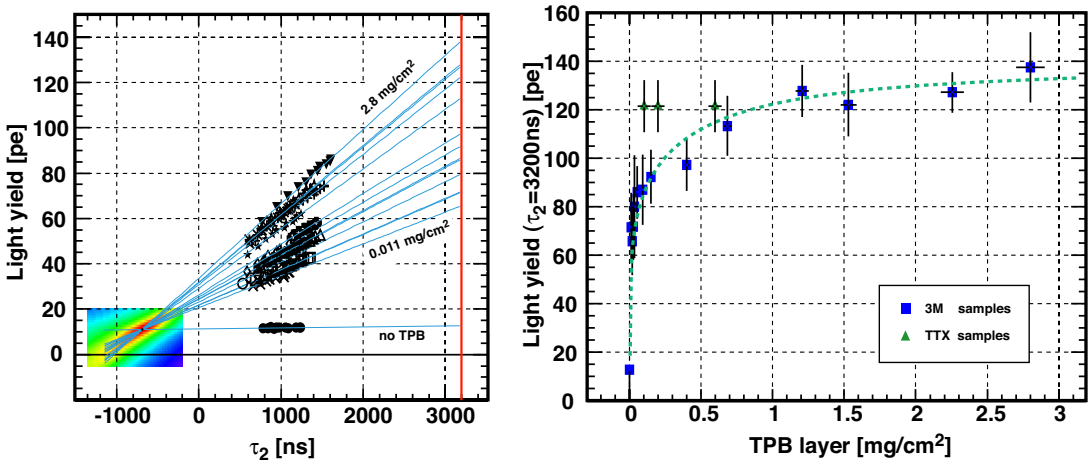

Figure 8. (left) Light yield in photoelectrons vs lifetime of the slow scintillation component for various thicknesses of TPB coatings on 3M ^{TM} foil; (right) Conversion efficiency (expressed as absolute yield in photoelectrons for an effective slow component of $3.2\,\mu$s) for the various thicknesses on 3M^{TM} foil compared to a few measurements of TTX foils.

within the errors with our measurements reported in ref. [8]. The x and y -positions of the point reflect a contribution of non 128 nm (but UV) light from fast light emission in NTP argon (roughly 17% at maximum gas purity [8]) and background of residual VUV sensitivity, respectively. The extrapolated (purity normalised) light yields (i.e. intersections of the lines with the value of $3.2\,\mu$s for τ_2) are plotted vs. the amount of TPB on the disks in figure 8(right). The result (errors from the line fits) is consistent with a saturation of VUV conversion efficiency above $1\,\mathrm{mg/cm^2}$(the dashed line is meant to guide the eye). A very similar result is achieved by not constraining the lines to a common intersection point but produces larger fluctuations.

The measurements were repeated on three TTX samples (triangles in figure 8(right)) showing a generally good performance and again a surprisingly weak dependance on the TPB layer thickness (consistent with the measurements of section 3.2).

3.4 Global efficiency of wavelength shifting and reflection

A schematic illustration of the argon gas apparatus which was used is shown in figure 9. This apparatus consisted of a sealed polyvinyl chloride (PVC) tube containing a 3" uncoated ETL PMT type 9302KB. An α-source located at the centre of a TPB coated reflector disk was placed within the tube at a variable distance from the PMT. Samples of either 3M ^{TM} foil or TTX cloth coated with TPB were placed around the interior walls of the tube. A gas delivery tube was inserted into the PVC chamber and 99.9999% pure argon gas at 1 bar flowed through the apparatus. The argon flow rate was used to control the argon purity. Measurements were taken for various TPB thicknesses between $0.2\,\mathrm{mg/cm^2}$ and $4.0\,\mathrm{mg/cm^2}$, which were deposited both via evaporation and spraying. Additionally, the distance between the α-source and the PMT was altered in order to investigate the effect of both the attenuation of light following multiple reflections and the reduction in direct VUV light incident on the PMT. The total number of photoelectrons collected by the PMT was analyzed for various distances d in the same way as described in section 3.3.

2009 JINST 4 P06001

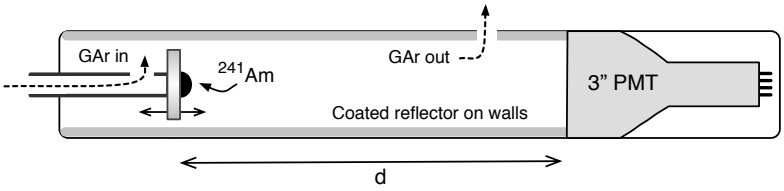

Figure 9. Schematic illustration of the argon gas apparatus used to determine the wavelength shifting and reflection efficiency as a function of distance d (ranging between 300 mm and 920 mm).

Evaporated coatings on 3M ^{TM} foils consistently underperformed TTX cloth irrespective of coating thickness. Thicker coatings on 3M ^{TM} foil yielded higher light collection whereas light collection from TPB evaporated on TTX substrates was found to be almost independent of thickness. The $0.2\,mg/cm^2$ TPB on TTX yielded within errors an identical result as for the $1.0\,mg/cm^2$ coating.

A visible difference between $0.2\,mg/cm^2$ sprayed and evaporated TPB on TTX cloth implied that spraying produces areas of low coating thickness and large inhomogeneity, while deposition via evaporation produces an uniform coating.

We concluded that it is advantageous to use evaporated TPB on TTX since smaller thicknesses of TPB may be used compared to 3M ^{TM} foil which requires between 4 and 20 times the thickness for comparative light collection. Thick coatings are far more brittle and fragile at low temperatures or when bent. This is especially true on 3M ^{TM} foil which, unlike TTX, does not provide any substantial keying to the surface.

TTX cloths coated by evaporation with $1.0\,mg/cm^2$ TPB were finally chosen for the ArDM reflector.

3.5 WLS coating on the PMT window

Another argon gas apparatus for direct light measurements was constructed with a similar aspect ratio as the full scale ArDM detector (figure 10). The experiment consisted of a sealed PVC tube containing a coated 3" ETL PMT type 9302KB. The PMT window was coated with TPB powder with thicknesses ranging from $0.02\,mg/cm^2$ to $2\,mg/cm^2$ via evaporation, spraying and application of a polymer matrix containing TPB. The sides and base of the PVC tube were covered with 3M ^{TM} foil reflector coated with $1\,mg/cm^2$ TPB powder by evaporation. TPB coated reflector walls were used as the ability of the window coating to shift VUV light is equally important as its ability to allow shifted visible light from the walls to penetrate. An α-source was positioned 10 cm away from the PMT window and argon gas was flowed continually.

TPB coating thicknesses above $2\,mg/cm^2$ are not recommended since the transparency of the PMT window coating to visible light would be significantly reduced. To avoid TPB crystallisation, deposition by spraying must be slow allowing for the evaporation of toluene. For polymer matrix coatings, crystallisation of TPB could be avoided with the addition of a plasticiser, which cross-links paraloid/polysterene chains with TPB, thus forming a rigid lattice while the solvent evaporates. Different coating thicknesses were tested for each one of the coating techniques (evaporation, spraying, paraloid and polystyrene matrix). From the different measurements, TPB coating

2009 JINST 4 P06001

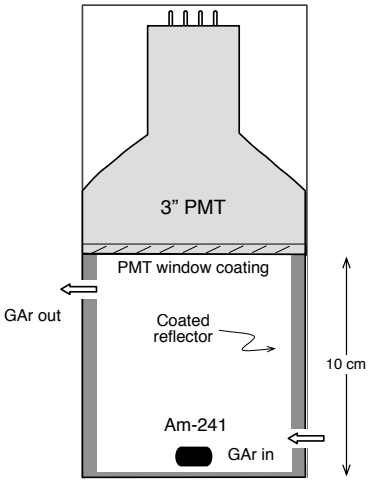

Figure 10. Schematic illustration of the argon gas apparatus used to determine the wavelength shifting efficiency of direct light incident on a TPB coated PMT.

by evaporation and TPB embedding in a polymer matrix (e.g. paraloid) were found to be the best within errors. The polymer matrix can be doped in a way that thin, crystal clear wavelength shifting coatings are produced. In general, PMT coating improves the total light collection in our geometry by about 30% (see also ref. [8]).

4 Application to the ArDM detector case

4.1 The large evaporation chamber

Driven by the experience gained with the different TPB deposition techniques, described in the previous sections, we built a stainless steel vacuum chamber large enough to house single reflector sheets of $120\times25\,\mathrm{cm}^2$ for the ArDM detector. The apparatus consists mainly of two parts, a horizontal tube with pumping connection on its closed end and a slide-in array of 13 crucibles mounted onto a Viton-sealed access flange. The crucibles are electrically connected in series for better uniformity and lower total supply current ($\approx$10 A). The reflector sheets are supported by 100 μm wires in a crescent arrangement for constant distance to the crucibles (see figure 11). An evaporation cycle was started by filling the crucibles with TPB powder and positioning the TTX reflector sheet on its support.

The reflector sheet surface was gently wiped by means of a grounded antistatic brush before the apparatus was closed and pumped. After reaching a typical pressure of 10^{-5} mbar the heating current was switched on and left running for about $3 \sim 5$ hours. The end of TPB evaporation was signaled by a small drop in the monitored vacuum pressure, presumably due to a small fraction of adsorbed water to the TPB powder (see figure 12).

After this preparation the sheets were inspected optically with a UV lamp (see figure 13) and stored in a clean cabinet until installation at the experiment. No degradation in the optical performance was observed while storing the reflector sheets up to 3 months.

2009 JINST 4 P06001

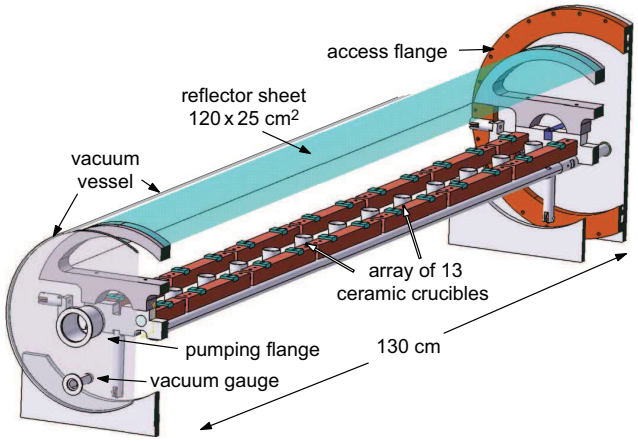

Figure 11. 3D sketch of the evaporation apparatus for the reflector sheets of the ArDM detector.

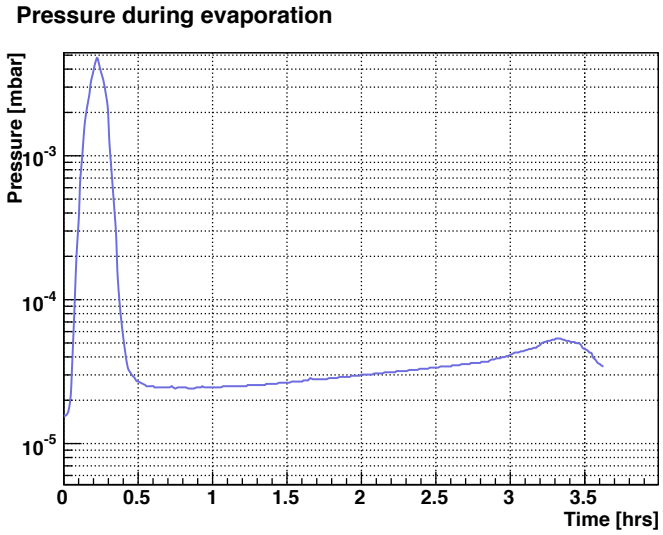

Figure 12. During the evaporation we constantly monitored the pressure of the evaporation vessel. The second peak shown in the graph, roughly after ≈ 3.3 hours, is interpreted as the moment in which no more TPB is remaining in the crucible.

4.2 Assembly of the wavelength shifting light reflectors in ArDM

The wavelength shifting side reflector is made of 15 overlapping panels, each of which is composed of a TTX reflector installed on 3M ^{TM} foil substrate which acts as a substrate, providing mechanical support and avoiding curling of the edges due to the high thermal shrinking coefficient of TTX. The panels were fixed on the first and last field shaper rings by means of teflon clips. The reflectors were installed such that they overlap slightly on their edges and produce a uniform reflector around the detector volume. UV lamp illumination results in a clear fluorescence (See figure 14).

The mechanical support of the photomultipliers can easily be adapted to support most of the commercially available 8" hemispherical PMTs. Bialkali photocathodes become insulant at low temperature; for this reason this kind of photomultipliers need an additional Pt deposition on the

2009 JINST 4 P06001

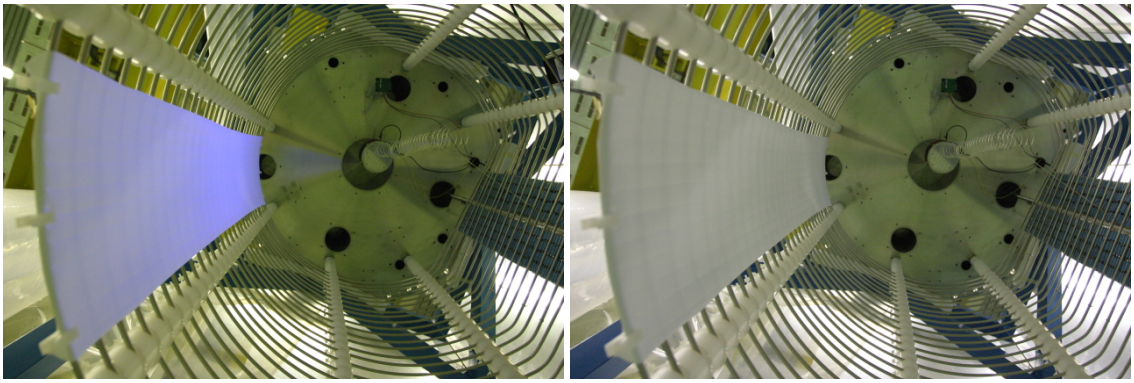

Figure 13. Optical inspection of one reflector sheet with a UV lamp (left) with illumination (right) without. The shifted light is readily visible on the illuminated reflector.

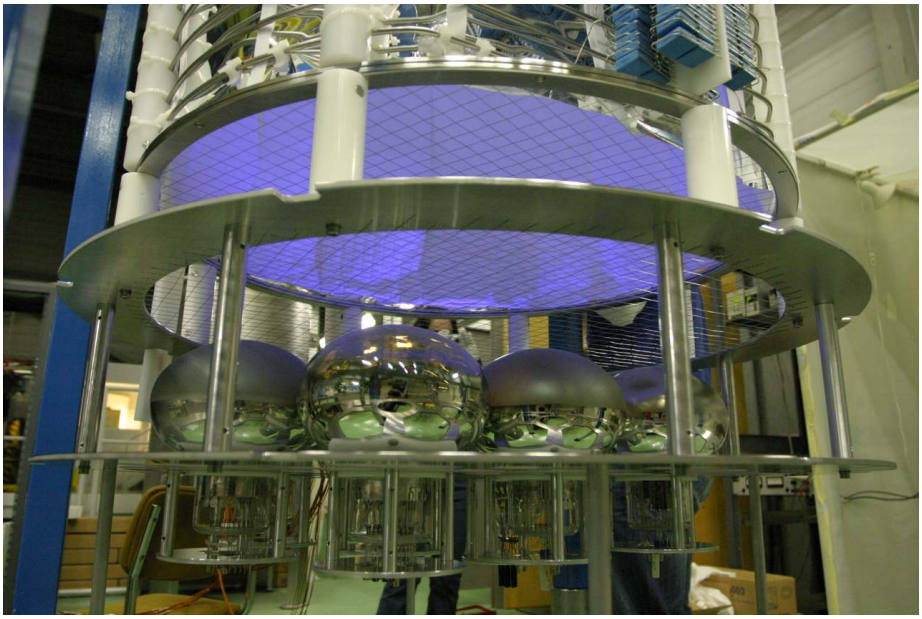

Figure 14. Picture of the light readout illuminated by UV light.

photocathode to restore the charges at cryogenic temperature with a drawback of a reduced quantum efficiency ($\simeq 2/3$ of the original). For the first test in gas and liquid argon 8 out of 14 cryogenic PMT modules were installed, as shown in figure 14: seven cryogenic Hamamatsu R5912(-02)MOD PMTs (five with 14 dynodes and two with 10 dynodes) and one ETL 9357 KFLB. Both types were previously studied at cryogenic temperatures [13, 29]. In addition, the PMT modules were tested in LAr (88K) with a blue LED ($\lambda_{pk} = 400\,\text{nm}$) light before coating and assembly in the experiment.

Ten PT-1000 temperature sensors, placed at different depth in the detector, allowed precise measurements of the inner temperature of the detector. The electric field generator chain and the E-Field protection grid, which protects the PMT surfaces from the high potential of the cathode, were installed but not used for these tests.

An ^{241}Am α-source (40 kBq) on a movable magnetic actuator and two blue LEDs were in-

2009 JINST 4 P06001

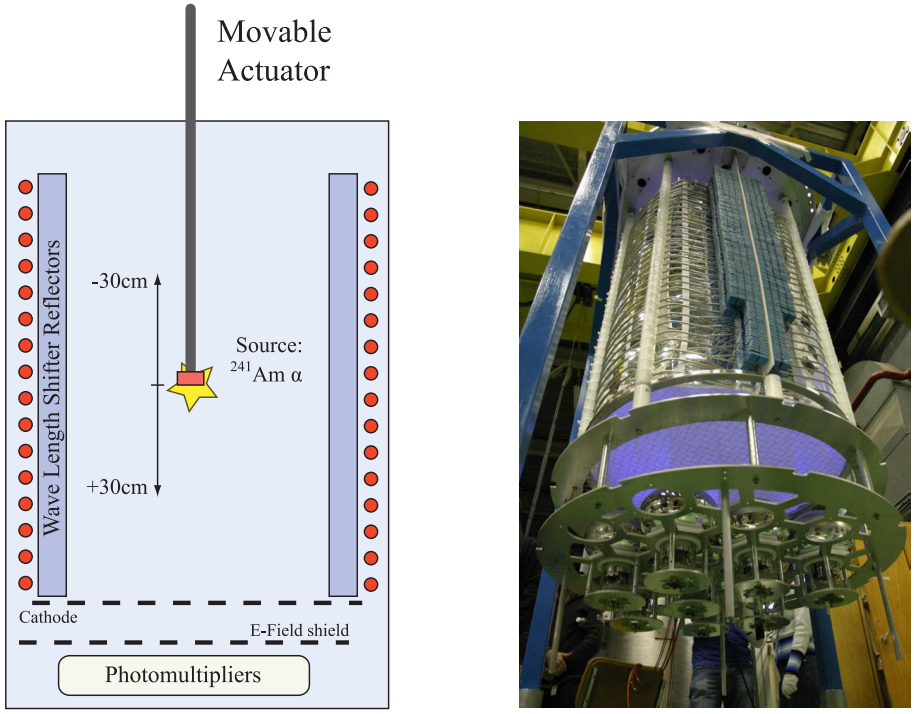

Figure 15. (left) Schematic of the setup used in the first tests; (right) Photograph of the assembled setup with internal UV light illumination.

stalled in the center of the main flange. An optical fiber was glued onto one of the LEDs; the other end of the fiber was mounted on the side of the movable source. In this way the source and the fiber can be moved vertically ± 30 cm from the center of the detector which allows the measurement of the light yield at different "event" positions. This source has a very thin metallic window which led to a reduction of the energy of the αs from 5.486 MeV to 4.5 MeV whose mean path is ≈ 3.5 cm in gaseous argon at 1.1 bar.

The signals of the PMTs are digitized by independent ADC channels (1GS/sec, 12bit resolution), triggered by a fast multiplicity signal from a programmable low threshold discriminator VME module. Data analysis is performed off-line, where low energy events from natural radioactivity as well as high energy cosmic ray muons can be easily discerned.

4.3 First measurement in gaseous argon

The test setup is schematized in figure 15 (left) while the picture of the assembled setup illuminated by UV light from inside is shown in figure 15 (right).

The setup was first closed and evacuated down to 10^{-5} mbar without baking. The dewar was then filled with pure gaseous argon[4] up to a pressure of 1.1 bar.

At the beginning we studied the performance of the photomultipliers: noise, dark count rate, and calibration curves were measured. Unfortunately two of the photomultipliers could be operated

[4]Argon N60 or ALPHAGAZ^{TM}2 ($> 99.9999\%$) argon, from Carbagas AG, (≤ 1 ppm).

2009 JINST 4 P06001

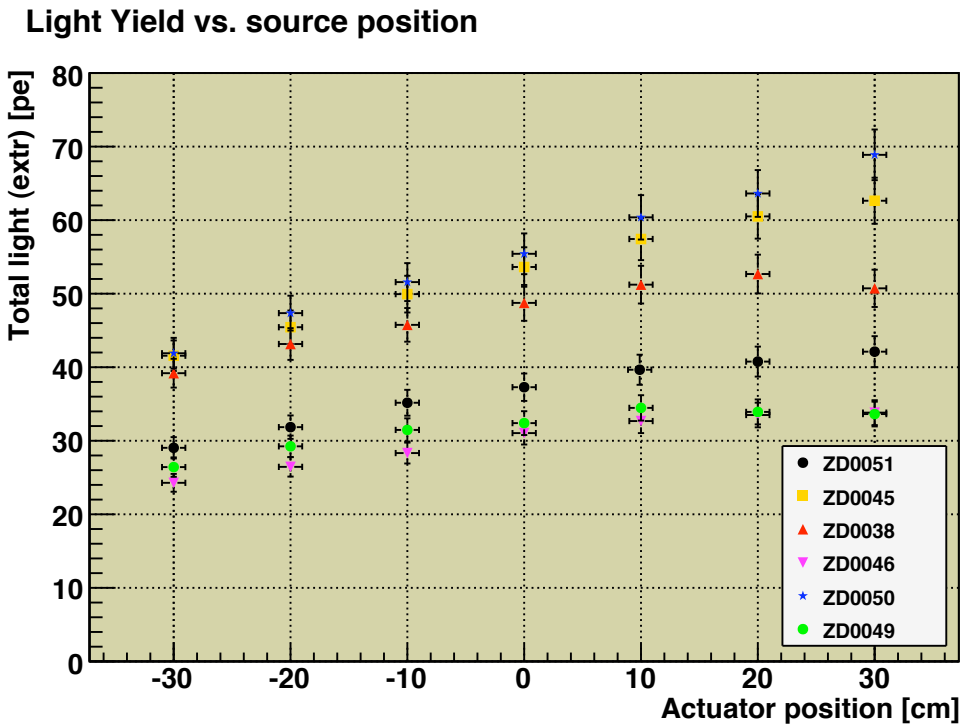

Figure 16. Average light detected with 6 PMT (labelled ZDxxxx) from 4.5 MeV α particle in GAr at 1.1bar for different source positions extrapolated to a slow component decay time of 3200ns.

only at low supply voltages (and consequently low gain) in gaseous argon because of sparking and could not be precisely calibrated (they will not be included in the following analysis).

At this point we acquired several series of data with the source at different position in the detector as can be seen in figure 16. Comparison of data with Monte Carlo is ongoing.

Argon gas was then left in for 1 month. For other 2 months the setup was operated with GAr at various pressures up to 2 bar. The setup was then again evacuated down to 10^{-5} mbar, filled with pure argon and the measurement was repeated.

We compared then the average pulse shapes of Am α-particles of two different data sets which had the same purity condition (same decay time of the slow component) and identical source position. The two data sets, as can be seen from figure 17, have the same amount of light within 1%. In conclusion there is no evidence of change in the light yield over a time interval of 3 months.

5 Conclusions

TPB can efficiently absorb VUV radiation from argon luminescence and re-emit at a wavelength which can be readily detected by bialkali photocathodes. In addition the wavelength shifting process is fast and insensitive to cryogenic temperatures. The optimum TPB deposition method was found to be vacuum evaporation which avoids crystallisation and coating inhomogeneities typically created during spraying. TPB coated TTX cloth was found to be the superior reflector when compared with 3M^{TM} foil due to its better light yield and greater tolerance to TPB layer thickness. Based on spectroradiometer measurements TPB coated TTX was found to have a reflectance

2009 JINST 4 P06001

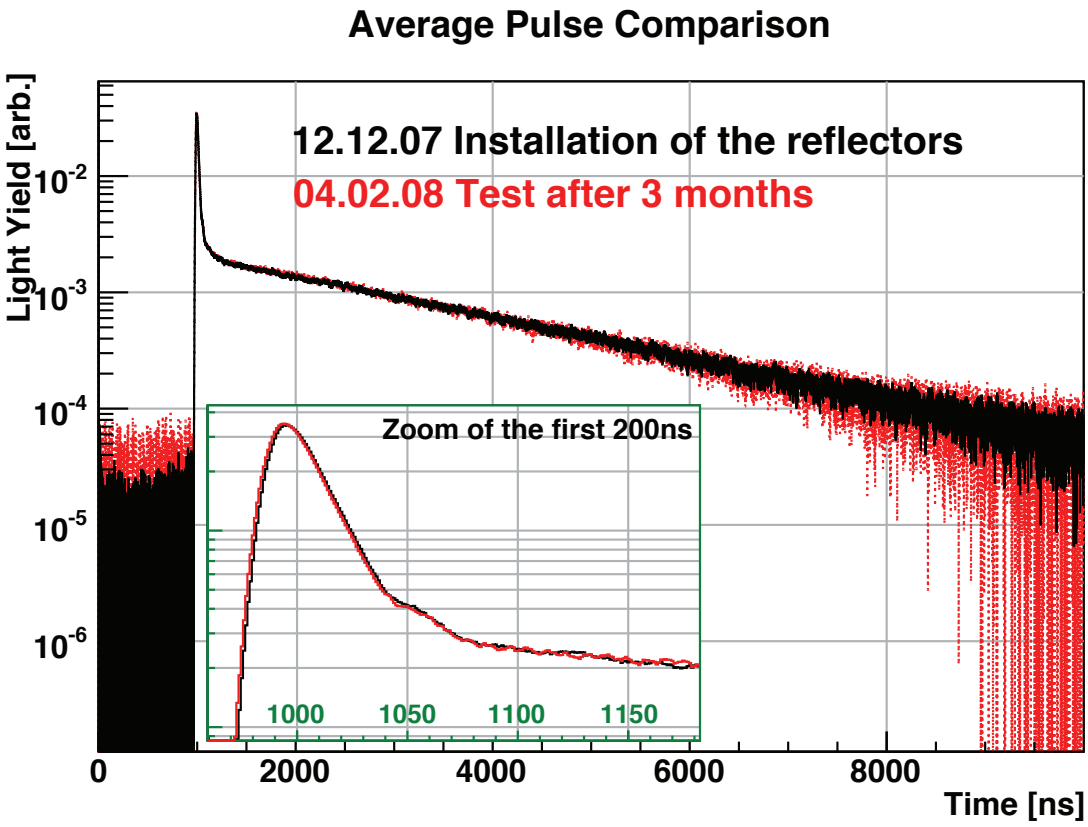

Figure 17. Signals from 4.5 MeV α particle (average pulse shape) in GAr at 1.1 bar for one of the photomultipliers. The black and red lines correspond to the signal measured just after the installation of the reflectors and after 3 months of operation, respectively.

coefficient at 430 nm close to 97% for all coating thicknesses. These measurements were used to define the parameters for the reflectors of the ArDM detector. The coating and reflector combination was chosen to be $1.0\,\mathrm{mg/cm^2}$ TPB deposited via evaporation on TTX cloth. Fifteen large $120 \times 25\,\mathrm{cm^2}$ TTX sheets were coated and assembled in the detector. Preliminary measurements in warm gas were performed with an ^{241}Am α-source. The light yields were measured at different time intervals, showing no evidence of aging in the time interval of 3 months.

Acknowledgments

This project is supported by ETH Zurich and the Swiss National Science Foundation (SNF).

References

[1] A. Rubbia, *ArDM: a ton-scale liquid argon experiment for direct detection of dark matter in the universe*, *J. Phys. Conf. Ser.* **39** (2006) 129 [hep-ph/0510320].

[2] ArDM collaboration, M. Laffranchi and A. Rubbia, *The ArDM project: a Liquid Argon TPC for Dark Matter Detection*, *J. Phys: Conf. Ser.* **65** (2007) 2014 [hep-ph/0702080].

[3] T. Doke, K. Masuda and E. Shibamura, *Estimation of absolute photon yields in liquid argon and xenon for relativistic (1 MeV) electrons*, *Nucl. Instrum. Meth.* **A 291** (1990) 617.

[4] S. Kubota, M. Hishida and J. Raun, *Evidence for a triplet state of the self-trapped exciton states in liquid argon, krypton and xenon*, *J. Phys.* **C 11** (1978) 2645.

[5] T.D. Strickler and E.T. Arakawa, *Optical Emission from Argon Excited by Alpha Particles: Quenching Studies*, *J. Chem. Phys.* **41** (1964) 1783.

[6] H. Langhoff, *The origin of the third continua emitted by excited rare gases*, *Opt. Commun.* **68** (1988) 31.

[7] W. Krötz et al., *Third excimer continuum of argon excited by a heavy-ion beam*, *Phys. Rev.* **A 43** (1991) 6089.

[8] C. Amsler et al., *Luminescence quenching of the triplet excimer state by air traces in gaseous argon*, 2008 *JINST* **3** P02001 [arXiv:0708.2621].

[9] S. Kubota et al., *Recombination luminescence in liquid argon and in liquid xenon*, *Phys. Rev.* **B 17** (1978) 2762.

[10] P. Benetti et al., *Detection of energy deposition down to the keV region using liquid xenon scintillation*, *Nucl. Instrum. Meth.* **A 327** (1993) 203.

[11] M.G. Boulay and A. Hime, *Technique for direct detection of weakly interacting massive particles using scintillation time discrimination in liquid argon*, *Astropart. Phys.* **25** (2006) 179.

[12] A. Badertscher et al., *Construction and operation of a Double Phase LAr Large Electron Multiplier Time Projection Chamber*, arXiv:0811.3384.

[13] A. Bueno et al., *Characterization of large area photomultipliers and its application to dark matter search with noble liquid detectors*, 2008 *JINST* **3** P01006 [arXiv:0711.3592].

[14] I.B. Berlman, *Handbook of Fluorescence Spectra of Aromatic Molecules*, Academic Press, New York and London (1965).

[15] W.M. Burton and B.A. Powell, *Fluorescence of Tetraphenyl-Butadiene in the Vacuum Ultraviolet*, *Appl. Optics* **12** (1973) 87.

[16] M. Grande and G.R. Moss, *An optimised thin film wavelength shifting coating for Cherenkov detection*, *Nucl. Instrum. Meth.* **215** (1983) 539.

[17] C.H. Lally, G.J. Davies, W.G. Jones and N.J.T. Smith, *UV quantum efficiencies of organic fluors*, *Nucl. Instrum. Meth.* **B 117** (1996) 421.

[18] D.N. McKinsey et al., *Fluorescence efficiencies of thin scintillating films in the extreme ultraviolet spectral region*, *Nucl. Instrum. Meth.* **B 132** (1997) 351.

[19] D.N. McKinsey et al., *Detecting ionizing radiation in liquid helium using wavelength shifting light collection*, *Nucl. Instrum. Meth.* **A 516** (2004) 475.

[20] ICARUS collaboration, S. Amerio et al., *Design, construction and tests of the ICARUS T600 detector*, *Nucl. Instrum. Meth.* **A 527** (2004) 329.

[21] P. Benetti et al., *First results from a dark matter search with liquid argon at 87-K in the Gran Sasso underground laboratory*, *Astropart. Phys.* **28** (2008) 495 [astro-ph/0701286].

[22] J.M. Flournoy, I.B. Berlman, B. Rickborn and R. Harrison, *Substituted tetraphenylbutadienes as fast scintillator solutes*, *Nucl. Instrum. Meth.* **A 351** (1994) 349.

[23] http://hepwww.rl.ac.uk/ukdmc/Radioactivity/Index.html.

2009 JINST 4 P06001

[24] A.I. Bolozdynya et al., *Using a Wavelength Shifter to Enhance the Sensitivity of Liquid Xenon Dark Matter Detectors*, *IEEE Trans. Nucl. Sci.* **55** (2008) 1453.

[25] G. Eigen and E. Lorenz, *A method of coating photomultipliers with wavelength shifters*, *Nucl. Instrum. Meth.* **166** (1979) 165.

[26] J.W. Keto, R.E. Gleason and G.K. Walters, *Production Mechanisms and Radiative Lifetimes of Argon and Xenon Molecules Emitting in the Ultraviolet*, *Phy. Rev. Lett.* **33** (1974) 1365.

[27] Optronic Laboratories Inc., http://www.olinet.com.

[28] H. Cabrera Cifuentes, *Test verschiedener Dichten von Tetraphenyl-Butadien auf 3M-Scheiben als Wellenlängergerschieber für das ArDM-Experiment*, Master Thesis, University of Zürich (2007).

[29] A. Ankowski et al., *Characterization of ETL 9357FLA photomultiplier tubes for cryogenic temperature applications*, *Nucl. Instrum. Meth.* **A 556** (2006) 146.

2009 JINST 4 P06001